PHYSICAL REVIEW B VOLUME 61, NUMBER 8 15 FEBRUARY 2000-II

Surface-state transitions of Si(111)-7×7 probed using nonlinear optical spectroscopy

Takanori Suzuki*
The Institute of Physical and Chemical Research (Riken) Wako, Saitama 351-0198, Japan
(Received 21 September 1999)

Surface second-harmonic generation of Si(111)-7×7 at RT reveals two surface-state transitions at 1.2 and 1.4 eV fundamental photon energies, in addition to the well-known two-photon resonance at 3.3 eV. A detailed analysis of the temperature-dependent spectral profile, combined with a separate sum-frequency generation and its gas-exposure measurement, attributes the 1.4-eV peak to the one-photon S_2-U_1 transition and the 1.2-eV peak to the two photon S_3-U_1 transition at 2.4 eV, which are fully consistent with the existing data on the surface states.

Surface states of Si(111)-7×7 have been the subject of numerous theoretical and experimental studies. Photoemission, electron energy loss, and scanning tunneling microscopy (STM) studies have revealed three occupied surface states and two unoccupied surface states.[1–5] Optical method (linear and nonlinear) has never definitely identified the optical transitions among the surface states of Si(111)-7×7. Linear optical methods, such as differential reflectance[6,7] and spectroscopic ellipsometry,[8] being in general accompanied by allowed bulk transitions, show a wide scattering of the surface-state transition energies.[7,8] The second-harmonic generation (SHG) and sum-frequency generation (SFG) spectroscopy, more sensitive in nature to the surface-state transitions, have been found to give a well-defined resonant profile.[9–12] The assignment of the transitions, however, still remains unclear mainly due to the limited wavelength range studied and to the interference among coexisting transitions.[9–13] It is further complicated by the fact that the two types of resonance enhancement, i.e., at the fundamental frequency (1ω) or at the second-harmonic frequency (2ω), are in general not readily discernible. The assignment of the SHG surface-state transitions is thus highly required for a further understanding of this surface.

Various techniques have shown the existence of three filled surface states of Si(111)-7×7 below/above the Fermi level: S_1 at ~ -0.2 eV, S_2 at ~ -0.8 eV, and S_3 at -1.8 eV, and two empty surface states: U_1 at ~ 0.5 eV and U_2 at 1.3–1.5 eV.[1–5] Within the dimer-adatom-stacking fault (DAS) model,[14] these states are attributed; S_1 to the adatom dangling bond, S_2 to the rest-atom dangling bond, S_3 to the back-bond of the adatoms and the corner-hole atoms, U_1 to the adatom dangling bond, and U_2 to the adatom back antibond. Inverse photoemission[3] (KRIPES) and angle-resolved photoemission spectroscopy[4,5] (ARUPS) have also reported the bandwidth and the band dispersion of the surface states. The temperature dependence of the surface states has also been studied by ARUPS.[15]

In our previous work,[16] we presented the temperature dependence of the nonlinear susceptibility of the surface-state transitions of Si(111)-7×7 for temperatures from room temperature (RT) to 1204 K. The strain-induced resonance around 3.3 eV, showing a clear increase in intensity with temperature, has been interpreted by thermal excitation of phonon modes localized at adatomic sites from an analysis of the SHG spectral profiles by using the classical anharmonic oscillator model.[16] In our successive work, we demonstrated the feasibility of the excitonic line-shape model for separating the surface-state transitions from other coexisting ones.[13] In this paper, we carried out an oxygen-exposure measurement of SHG and SFG at several wavelengths. The analysis of the coverage and temperature dependence of SHG and SFG has guided us to uniquely assign the surface-state transitions, which are fully consistent with the existing data on the surface states.

The details of our observation of the SHG spectra of Si(111) have been described elsewhere.[16] In our experiment, the anisotropic component of the second-order susceptibility χ_{xxx} was measured by detecting the generated SHG photons with *s* polarization in response to the incident beam at near-normal incidence with *p* polarization, which is perpendicular to the crystal $[2\bar{1}1]$ direction. An optical parametric oscillator/amplifier system at a 10 Hz repetition rate with a nominal bandwidth of 0.3 cm^{-1} was used as a pumping laser. For an SFG measurement, we used *p* polarized second harmonics (0.532 μm) of 10 mJ output energy from another synchronously operated *Q*-switched YAG laser directed collinearly with the tunable laser. The Si sample, cut from a *B*-doped commercial wafer with a resistivity of 0.4 Ω cm, was set in an ultrahigh vacuum chamber and cleaned by resistive heating to 1420 K. Oxygen dosing was done by backfilling the chamber with O_2. The SHG and SFG spectra normalized against the incident laser energy are shown for $|\chi_{xxx}|^2$ by correcting for the Fresnel factors.[16]

Figure 1 reproduces $|\chi_{xxx}|^2$ of Si(111)-7×7 obtained by SHG as a function of the pumping photon energy for several temperatures.[16] The lines showing the fits to the experimental data will be discussed later. The peak around 1.65 eV (1.65-eV peak) has been attributed to a strain-induced two-photon resonance of the E_0' interband transition in the surface layers of bulk silicon.[16,17] The broad feature of 7×7 is known to originate from the resonant enhancement of SHG by the dangling bond states,[9–12] which appears to be composed of two components around 1.2 eV (1.2-eV peak) and 1.4 eV (1.4-eV peak) in Fig. 1(a). The 1.4-eV peak decreases its amplitude much faster with temperature than that of the 1.2-eV peak [Fig. 1(a)–1(c)], and is not recognizable in Figs. 1(d)–1(g). Our observation of the surface-state transitions

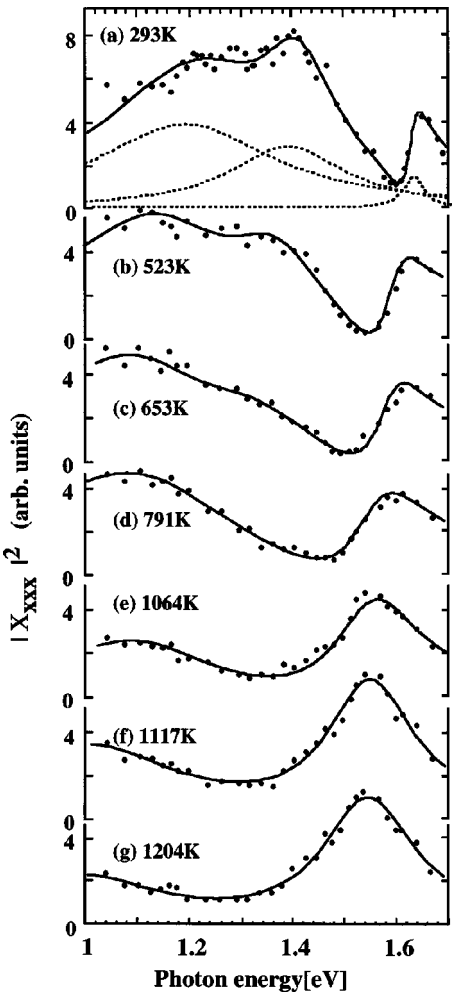

FIG. 1. Wavelength dependence of the second-order nonlinear susceptibility χ_{xxx} of Si(111) for several temperatures. (a)–(e) for 7×7, and (f), (g), for ''1×1.'' The solid lines are the fitting results using the excitonic line shape. The dotted lines in (a) are the calculated individual components.

shows an unusual feature in that a single and broad peak centered at 1.3 eV reported previously[9–12] is clearly separated into two components. Besides, the 1.15-eV peak reported by Pedersen and Morgen[11] was never observed. The two panels (f) and (g), just above the phase-transition temperature $T_c \sim 1103$ K, corresponds to the SHG spectra of ''1×1.''

Figure 2 is the SFG spectra obtained at RT together with a reproduction of Fig. 1(a) for comparison. SFG noises were much larger than those of SHG, which were introduced by the timing and intensity fluctuations of the fixed wavelength laser and by a low efficiency of our detection system in the UV region. The SFG spectra showing a broad resonance around 1.2 eV without any enhanced peak at 1.4 eV had guided us to incorrectly assign the 1.2-eV peak of SHG to a one-photon resonance.[13]

The variation of SH and SF signals with O_2 exposure at a pressure of 2×10^{-8} Torr at RT is shown in Fig. 3 for a few selected wavelengths, where the oxygen exposure is expressed in units of L (1 L= 10^{-6} Torr s). The SHG data with a rapid decrease to zero are consistent with previous measurements.[11,18,19] The SFG spectra, however, shows only

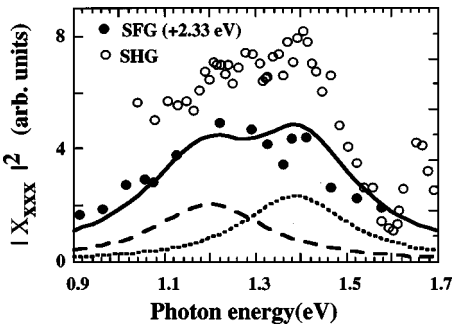

FIG. 2. The SFG spectra of 7×7 at RT taken by mixing with a fixed wavelength laser at 2.34 eV, with a reproduction of Fig. 1(a) for comparison. Calculated SFG spectra are shown by the solid line, with dotted and dashed lines separately showing the SS and BG contributions, respectively (see text for details).

a partial decrease followed by a much slower increase to a wavelength-dependent saturation level. Thus, the sensitivity to oxidation is clearly different between SHG and SFG.

The dangling-bond-derived surface states are quenched by most chemisorbates.[9,18,19] The coverage dependence of SHG has been well described by expressing the nonlinear susceptibility $\chi_s^{(2)}(\theta)$ as a sum of a strong coverage-dependent surface-state (SS) contribution proportional to the number of dangling bonds $\chi_{s,db}^{(2)}$ and a weakly coverage-dependent background (BG) contribution $\chi_{s,BG}^{(2)}$, as[9]

$$\chi_s^{(2)}(\theta)=\chi_{s,db}^{(2)}(1-\alpha\theta)+\chi_{s,BG}^{(2)}(\theta), \tag{1}$$

where α incorporates the nonlocal influence of adsorption on the surface electronic states, which turned out to be unity in this work. The oxide coverage θ can be described by an oxygen exposure d and a reactive coefficient k as $\theta(d)=1-\exp(-kd)$. The phase ϕ of $\chi_{s,BG}^{(2)}$ relative to $\chi_{s,db}^{(2)}$ is also obtained in the fitting procedure. This model reproduced well the SHG adsorption curves as shown by the solid lines in Figs. 3(a)–3(d) with $k\sim0.4$ L^{-1} and $\phi\sim160°$. The obtained

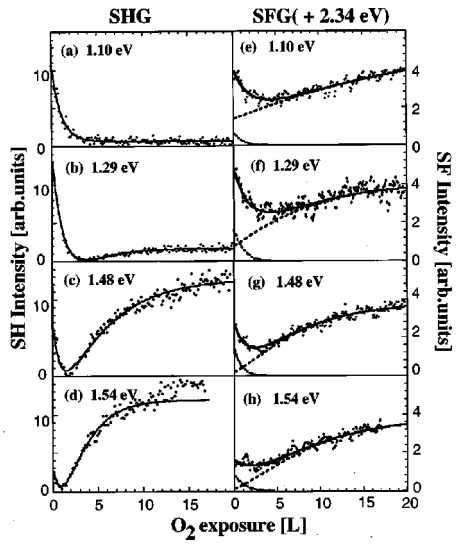

FIG. 3. Oxygen-exposure experiment for SHG and SFG obtained at several wavelengths. The solid lines are the best-fit curves with the dotted and dashed lines separately showing the SS and BG contributions, respectively.

phase is sufficiently close to the directly measured value of 132° for a sample with a 30 L oxygen exposure.[13] The BG contribution has been suggested to be mainly the tail of the strain-induced resonance at 3.3 eV.[9,11] The reactive coefficients obtained for SFG by using Eq. (1) were about half of SHG values, which disagrees with our adsorption model where a similar value is expected both for SHG and SFG. When we added to Eq. (1) a coverage-dependent BG contribution in proportion to $[1-\exp(-k_b d)]$, $k\sim 0.4\ \mathrm{L}^{-1}$ was also obtained for SFG, which reasonably made us conclude that the slower increase observed in SFG is due to a coverage-dependent BG contribution. The solid lines in Figs. 3(e)–3(h) are thus obtained with the dotted and dashed lines, separately indicating the fast-decay SS contribution and the coverage-dependent BG contribution, respectively. Note that the BG contribution for 7×7 is dominant at lower photon energy [Fig. 3(e)], while the SS contribution is most dominant around 1.48 eV [Fig. 3(g)]. Note also that the SS contribution with a sum-frequency energy of 3.8 eV, much larger than the 3.4 eV direct band gap, is of the 1ω resonance type, while the BG contribution to SFG increasing with oxygen coverage is of a sum-frequency resonance type. Thus, the main contribution to SHG in Fig. 1 can be interpreted as a 1ω resonance for the 1.4-eV peak and a 2ω resonance for the 1.2-eV peak.

Now that we know the resonance type of the main contribution to the SH response shown in Fig. 1, the interference among different transitions can be resolved. The excitonic line shape has been discussed in detail in Refs. 20 and 21. We simply use the excitonic line shape in our analysis of the SHG and SFG spectra, although we are unaware of the character[21] of the SS transition. In this model, the SHG spectral profile is reduced by a coherent superposition of the second-order nonlinear susceptibility of 1ω and 2ω resonances, as[13,20]

$$\chi_s^{(2)}(2\omega)\propto\sum_{k,l}\left\{\frac{f_k\exp(i\varphi_k)}{(\omega-\omega_k+i\Gamma_k/2)}+\frac{f_l\exp(i\varphi_l)}{(2\omega-\omega_l+i\Gamma_l/2)}\right\},\quad(2)$$

where ω_j is the resonance frequency, Γ_j is a damping frequency (FWHM of the resonance), with the amplitudes f_k and f_l, and phases φ_k and φ_l. Phases are introduced for each resonance in order to describe other resonant/nonresonant contributions.[13]

The solid lines in Fig. 1 are the fitting results for three resonances given by (2) ($k=1$, $l=2$), which relates one to a 1ω resonance around 1.4 eV, another to a 2ω resonance around 1.2 eV, and the other to a 2ω resonance around 1.65 eV. In the fitting procedure, the same phase φ is assumed for the two SS transitions leaving the relative phase of the 1.65-eV peak as a fitting parameter. All others are used as fitting parameters. The SHG spectra are reproduced well by the three-resonance model for (a)–(c). Since the 1.4-eV peak already becomes negligible in (d), we used the two-resonance model ($k=0$, $l=2$) for fitting (d)–(g). The solid lines in Fig. 1 are thus obtained with dotted lines in (a) showing the individual contributions. The fitting results are shown in Fig. 4. Although a different SS transition type is employed compared to Ref. 16, the main features of the 1.65-eV peak remain the same; only with a slightly smaller activation energy of 62 meV (from 75 meV), which favors

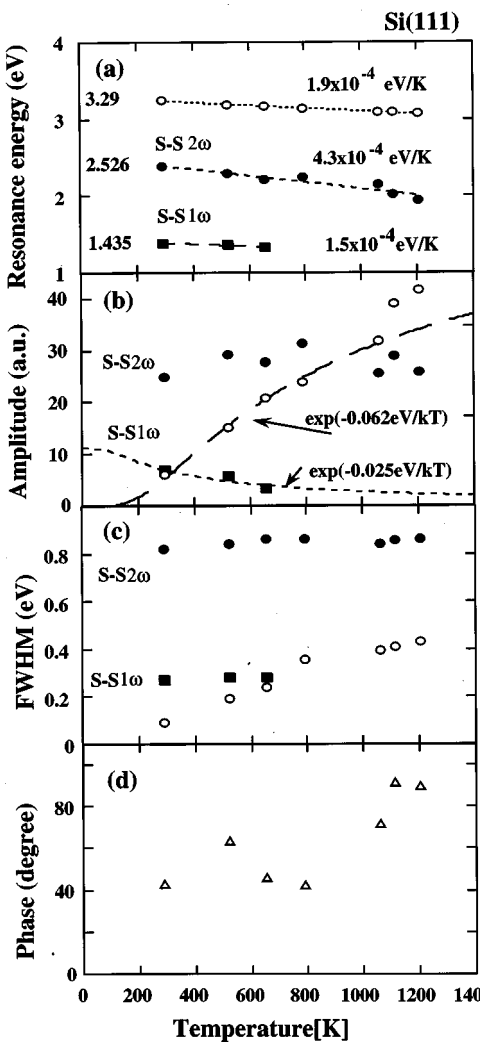

FIG. 4. Parameters obtained by fitting the SHG data in Fig. 1 by the excitonic line shape.

our interpretation in terms of excitation of surface phonon modes at 17 THz (68 meV) or 12.5 THz (50 meV).[16]

The surface-state transitions in Fig. 4(a) show a redshift with a temperature coefficient of 4.3×10^{-4} eV/T (1.2-eV peak) and 1.5×10^{-4} eV/T (1.4-eV peak), which is roughly in agreement with 1.9×10^{-4} eV/T (1.65-eV peak) and the bulk E_0'/E_1 value of 1.7×10^{-4} eV/T which has been associated with the lattice expansion and the electron-phonon interaction.[21] The amplitude and width of the SS transitions show a different temperature dependence as compared with the 1.65-eV peak. While the 1.2-eV peak has a temperature-independent amplitude and width (0.8 eV), the 1.4-eV peak with a temperature-independent width (0.3 eV) decreases its amplitude with a rate corresponding to an activation energy of ~25 meV. The 7×7-''1×1'' phase transition appears only as a jump of the surface-state transition amplitude, showing a similar electronic structure in both phases in spite of a different surface atomic geometry.

Although all transitions, among surface states and between surface states and bulk conduction/valence bands, are in principle allowed for SHG at silicon surfaces,[7] we may first look for transitions among the surface states for the observed well-defined two peaks. The 1.4-eV peak may be as-

signed to the $S_2 \rightarrow U_1$ transition because of the matching with the known energy level spacing of ~1.3 eV. It also agrees with the 1.45 eV estimated by the tight-binding calculation.[7] The charge transfer from the adatoms will also ensure a significant population of S_2. Moreover, our SHG observation of decreasing intensity of the 1.4-eV peak with temperature is in accord with the ARUPS observation of disappearance of the surface state at -0.8 eV below the Fermi energy (corresponding to S_2) above 250 °C reported by Yokotsuka *et al.*[15] The initial state of the 1.2-eV peak may then be S_3, since S_2 can be discarded because of its temperature-independent amplitude. The $S_3 \rightarrow U_1$ transition with an energy level separation of ~2.3 eV, then matches well with the two-photon transition at 2.4 eV. Thus, both resonances can be assigned to the transitions among the known surface states.

The above assignment is further supported by the available widths of the surface states; a bandwidth of larger than 0.5 eV and a dispersion of 0.2 eV for U_1 obtained by KRIPES (Ref. 3) and a dispersion of less than 0.15 eV for a flat band S_2 obtained by ARUPS.[5] The 0.3-eV width obtained for the $S_2 \rightarrow U_1$ transition [Fig. 4(c)] gives ~0.3 eV for the total width of U_1, since the linewidth is determined mainly by U_1 having a larger width. This width, more accurate in nature, is consistent with the above KRIPES data if their instrumental bandwidth of as large as 0.35 eV,[3] is taken into account. The broad and temperature-independent width of 0.8 eV of the 1.2-eV peak then must be explained by S_3, for which a bandwidth of 0.3 eV is reported.[5] It is to be noted that the SHG width reflects both the bandwidth and dispersion since a pure optical method cannot resolve the band dispersion. Although numerical specifications for the dispersion of S_3 are not given, a dispersion of ~0.4 eV seen in Fig. 8 of Ref. 5 gives a total width of 0.7 eV for S_3. The SHG width of 0.8 eV then reasonably matches the $S_3 \rightarrow U_1$ transition width if we take into account the U_1 width of ~0.3 eV.

The background SFG signal is likely related to the SHG resonance at 3.6 eV, recently reported by Erley and Daum[20] for an interband transition at the Si(100)- SiO_2 interface and assigned to Si atoms without T_d lattice symmetry, because of a coincidence of the transition energy. The SFG signal of similar origin may also be expected for 7×7 due to the lattice distortion inherent to this reconstruction. Figure 3 shows a redshift for the SFG BG contribution of 7×7 compared with that of the oxidized surface. This, possibly related to a different amount of distortion, also contributes to the observed coverage dependence of the BG contribution. The ratios of the BG and SS contributions in Fig. 3 and the results in Fig. 4 for the SS transitions can also roughly reproduce the SFG spectra in Fig. 2, as shown by the solid line for the BG resonance energy of 3.55 eV and a FWHM width[20] of 0.3 eV. The dotted and dashed lines represent the separated BG and SS contributions, respectively.

Our assignment of the SHG resonances; the $S_2 \rightarrow U_1$ transition for the 1.4-eV peak and the $S_3 \rightarrow U_1$ transition for the 1.2-eV peak, is thus consistent with the available photoemission and STM data on the Si(111)-7×7 surface states. The 1ω SS transition is consistent with the transient population grating in the U_1 state formed by excitation at ~1.5 eV reported by Höfer *et al.*,[22,23] while the assignment of the SHG broad resonance around 1.3 eV to the $S_2 \rightarrow U_1$ transition suggested by Pedersen *et al.*[11,12] is clearly not consistent with our findings.

The origin of the temperature dependence of S_2 has not been identified.[15] Changes in the symmetric property of the surface states by phonon excitation[16] do not describe the temperature dependence observed by photoemission, nor does the electric-field induced SHG,[24] even with a coincidence of the disappearance of the surface band bending at some 800 K estimated for our sample with a doping concentration of 10^{17} cm^{-3}.[25] At present, we do not have a conclusive explanation for the decrease of the 1.4-eV peak with temperature.

We thank S. Kogo and M. Kaneuchi for technical assistance, and Dr. M. Tsukakoshi, Dr. M. Aono, and Dr. A. Misu for helpful discussions. Stimulating discussions with Dr. U. Höfer are gratefully acknowledged.

*FAX: 048-462-4652. Electronic address: tsuzuki@postman.riken.go.jp

[1] R. J. Hamers, R. M. Tromp, and J. E. Demuth, Phys. Rev. Lett. **56**, 1972 (1986).
[2] J. Demuth *et al.*, Phys. Rev. Lett. **51**, 2214 (1983).
[3] J. M. Nicholls and B. Reihl, Phys. Rev. B **36**, 8071 (1987).
[4] R. I. G. Uhrberg *et al.*, Phys. Rev. B **31**, 3805 (1985).
[5] P. Martennsson *et al.*, Phys. Rev. B **36**, 5974 (1987).
[6] K. Alameh and Y. Borensztein, Surf. Sci. **251/252**, 396 (1991).
[7] C. Noguez, A. I. Shkrebtii, and R. Del Sole, Surf. Sci. **331/333**, 1349 (1995), and references therein.
[8] Z. Hammadi *et al.*, Surf. Sci. **341**, 202 (1995).
[9] U. Höfer, Appl. Phys. A: Mater. Sci. Process. **63A**, 533 (1996).
[10] T. Suzuki *et al.*, in *International Quantum Electronics Conference, 1996*, OSA Technical Digest Series (Optical Society of America, Washington, D.C., 1996), p. 33.
[11] K. Pedersen and P. Morgen, Phys. Rev. B **52**, R2277 (1995); **53**, 9544 (1996).
[12] K. Pedersen and P. Morgen, Surf. Sci. **377/379**, 393 (1997).
[13] T. Suzuki *et al.*, Appl. Phys. B: Lasers Opt. **68**, 623 (1999).
[14] K. Takayanagi *et al.*, J. Vac. Sci. Technol. A **3**, 1502 (1985).
[15] T. Yokotsuka *et al.*, Solid State Commun. **39**, 1001 (1981); **46**, 401 (1983).
[16] T. Suzuki *et al.*, Phys. Rev. B **59**, 12 305 (1999).
[17] W. Daum *et al.*, Phys. Rev. Lett. **71**, 1234 (1993).
[18] P. Bratu, K. L. Kompa, and U. Höfer, Phys. Rev. B **49**, 14 070 (1994).
[19] A. A. Shklyaev and T. Suzuki, Phys. Rev. Lett. **75**, 272 (1995).
[20] G. Erley and W. Daum, Phys. Rev. B **58**, R1734 (1998).
[21] P. Lautenschlager *et al.*, Phys. Rev. B **36**, 4821 (1987).
[22] U. Höfer, Appl. Phys. B: Lasers Opt. **68**, 383 (1999).
[23] G. A. Schmitt, P. Bratu, and U. Höfer (private communication).
[24] J. I. Dadap *et al.*, Phys. Rev. B **56**, 13 367 (1997).
[25] *Semiconductors*, edited by O. Madelung, Landolt-Börnstein New Series, Group III, Vol. 17, Pt. a (Springer-Verlag, Berlin, 1982).